Journal of Sound and Vibration 328 (2009) 148–155

Contents lists available at ScienceDirect

Journal of Sound and Vibration

journal homepage: www.elsevier.com/locate/jsvi

Second-harmonic generation of practical Bessel beams

Jin H. Huang [a,*], Desheng Ding [b,c], Yin-Sung Hsu [d]

[a] Department of Mechanical and Computer-Aided Engineering, Feng Chia University, Taichung 40724, Tiawan, ROC
[b] College of Engineering, Feng Chia University, Taichung 40724, Taiwan, ROC
[c] Department of Electronic Engineering, Southeast University, Nanjing 210096, People's Republic of China
[d] Department of Water Resources Engineering and Conservation, Feng Chia University, Taichung 40724, Republic of China

ARTICLE INFO

Article history:
Received 5 December 2008
Received in revised form
1 August 2009
Accepted 3 August 2009
Handling Editior: L.G. Tham
Available online 31 August 2009

ABSTRACT

A fast Gaussian expansion approach is used to investigate fundamental and second-harmonic generation in practical Bessel beams of finite aperture. The analysis is based on the integral solutions of the KZK equation under the quasilinear approximation. The influence of the medium's attenuation on the beam profile is considered. Analysis results show that the absorption parameter has a significant effect on the far-field beam profile of the second harmonic. Under certain circumstances, the second harmonic of a practical Bessel beam still has the main properties of an ideal Bessel beam of infinite aperture when it propagates within its depth of field.

1. Introduction

Because of the "diffraction-free" feature, Bessel beams and some of more general diffraction-free beams, such as X wave beams, have long been widely investigated in the relevant specialties of physics, such as optics and acoustics [1–21]. In theory, an ideal Bessel beam with infinite extent and energy can propagate to infinity without any spreading. However, such an ideal Bessel beam is impossible to realize experimentally. In practice, the aperture of a physically realizable Bessel beam is always finite. Even so, the beam has a very large depth of field in which the beam profile basically remains a Bessel function distribution with little spreading. Recently, the nonlinear propagation of Bessel beams has attracted considerable interest, due to its potential applications such as ultrasonic harmonic imaging and nonlinear optics [6,7,14–21]. In many primary studies, the theoretical analysis is made under oversimplified assumptions. Obviously, it is difficult for these assumptions to satisfy the physical reality that the aperture of the Bessel beam is finite and the absorption (and dispersion) of media is usually non-negligible. As Arlt et al. noticed [7], if the reality is not taken into consideration, the theoretical deduction will probably disagree with experiment, and might even lead to errors in stark contrast to experimental results.

In this paper, we investigate the fundamental and second-harmonic generation of the Bessel beam under practical conditions; we consider the finiteness of the beam aperture and the absorption effect of media. Our analysis is based on the integral solutions to the KZK parabolic nonlinear wave equation [22–24] under the quasilinear approximation. A Gaussian expansion technique is applied to evaluate these integrals for the fundamental and second-harmonic fields [25–34]. The numerical results show that for a practical finite aperture Bessel beam, as long as its aperture contains many lobes of the Bessel function profile, the second-harmonic beam maintains the same main characteristics as are found in the infinite aperture case. The absorption effect is also analyzed with regard to the radial pattern of the Bessel second-harmonic beam.

* Corresponding author. Tel.: +886 4 24518951; fax: +886 4 24516545.
E-mail address: jhhuang@fcu.edu.tw (J.H. Huang).

0022-460X/$ - see front matter
doi:10.1016/j.jsv.2009.08.004

2. Basic field integrals and Gaussian expansion

Here we provide only the linear and quasilinear solutions to the KZK nonlinear parabolic wave equation and their alternative forms in dimensionless variables. The detailed derivations of these formulas can be found in some articles and textbooks [22–34]. We assume that an axial-symmetric sound source, with an angular frequency ω and a characteristic radius a, oscillates harmonically in time, and the direction of the beam propagation is along the z-axis. In the quasilinear approximation, the linearized solution to the equation for the fundamental pressure field is [22–34]

$$p_1(\xi,\eta;\tau) = \mathrm{Re}[p_0 \mathrm{e}^{-\mathrm{i}\tau}\bar{q}_1(\xi,\eta)] \tag{1a}$$

where

$$\bar{q}_1(\xi,\eta) = \frac{2}{\mathrm{i}\eta}\mathrm{e}^{-\bar{\alpha}_1\eta}\int_0^\infty \exp\left(\mathrm{i}\frac{\xi^2+\xi'^2}{\eta}\right)J_0\left(\frac{2\xi\xi'}{\eta}\right)\bar{q}_1(\xi')\xi'\,\mathrm{d}\xi' \tag{1b}$$

and the second-harmonic component is

$$p_2(\xi,\eta;\tau) = \mathrm{Re}\left\{-2p_0^2\frac{\beta k^2a^2}{\rho c_0^2}\mathrm{e}^{-\mathrm{i}2\tau}\bar{q}_2(\xi,\eta)\right\} \tag{2a}$$

where

$$\bar{q}_2(\xi,\eta) = \frac{1}{2}\mathrm{e}^{-\bar{\alpha}_2\eta}\int_{\eta'=0}^{\eta}\int_{\xi'=0}^{\infty}\mathrm{e}^{\bar{\alpha}_2\eta'}\frac{\xi'}{\eta-\eta'}\exp\left(\mathrm{i}2\frac{\xi^2+\xi'^2}{\eta-\eta'}\right)J_0\left(\frac{4\xi\xi'}{\eta-\eta'}\right)\bar{q}_1^2(\xi',\eta')\,\mathrm{d}\xi'\,\mathrm{d}\eta' \tag{2b}$$

Here $\xi = r/a$ and $\eta = z/z_0$ are the radially and axially dimensionless coordinates, $z_0 = ka^2/2$ is the Rayleigh distance, and $k = \omega/c_0$ is the wavenumber. Correspondingly, the notations r and z denote the radial and axial coordinates. For a real (finite size) transducer, a may be taken as its radius. The meaning of the other notations is the same as explained in most Refs. [22–34], i.e., $\tau = \omega(t - z/c_0)$, p and $p_0 = \rho_0 u_0 c_0$. Here p is the sound pressure, t the time, c_0 the small signal sound speed, and ρ_0 the ambient density of the medium. Furthermore, u_0 is the characteristic value of the normal velocity on the source, β is the nonlinearity coefficient and $\bar{\alpha} = z_0\alpha$, with the absorption coefficient α at the angular frequency ω (the dispersion effect, if considered, may be introduced as the imaginary part of α) [22–24]. In the integral of the right-hand side of Eq. (1b), $\bar{q}_1(\xi')$ is the source function in the plane $\eta' = 0$. On the basis of Eq. (2b), the second-harmonic generation in the quasilinear approximation is interpreted as a sound field radiated by a volume distribution of virtual sources whose strengths are proportional to $\bar{q}_1^2(\xi,\eta)$ [24]. Eqs. (1b) and (2b) are the complex-valued pressure amplitudes in dimensionless form. In these equations, the quantities $\bar{\alpha}_1$ and $\bar{\alpha}_2$ are the absorption coefficients by measuring the Rayleigh distance at the frequencies $\omega_1 = \omega$ and $\omega_2 = 2\omega$.

In the most general case, the integral solutions (1b) and (2b) must be numerically evaluated for the fundamental and second-harmonic fields of an arbitrary distributed source. This numerical evaluation is relatively time-consuming, especially for Eq. (2b), a three-dimensional and strongly oscillatory integral. Fortunately, the Gaussian expansion technique [25–34] is particularly useful to simplify these integrals. In what follows, we briefly present an outline of this approach and apply it to analysis of the fundamental and second-harmonic fields of the Bessel beams of finite aperture.

When an axial-symmetric source function is expanded into

$$\bar{q}_1(\xi) = \sum_{k=1}^{N} A_k \exp(-B_k\xi^2) \tag{3}$$

the fundamental field of Eq. (1b) is reduced to calculation of simple Gaussian functions

$$\bar{q}_1(\xi,\eta) = \sum_{k=1}^{N}\frac{A_k}{1+\mathrm{i}B_k\eta}\exp\left(-\frac{B_k\xi^2}{1+\mathrm{i}B_k\eta}\right) \tag{4}$$

For a given source function, a set of A_k and B_k, the expansion and Gaussian coefficients, may be determined by computer optimization or the other methods [25,29].

Correspondingly, the second-harmonic sound beam of Eq. (2b) is evaluated by [32–34]

$$\bar{q}_2(\xi,\eta) = \int_{\eta'=0}^{\eta}\sum_{k=1}^{N}\sum_{j=1}^{N}A_kA_j\bar{q}_2(\xi,\eta;k,j;\eta')\,\mathrm{d}\eta' \tag{5}$$

where

$$\bar{q}_2(\xi,\eta;k,j;\eta') = \frac{1}{4}\exp\left(-\frac{s_1}{r_1}\xi^2 - \bar{\alpha}_2\eta\right)\frac{1}{r_1\eta'+r_2}\exp\left[\frac{s_2\xi^2}{r_1(r_1\eta'+r_2)} + (\bar{\alpha}_2 - 2\bar{\alpha}_1)\eta'\right] \tag{6}$$

and

$$r_1 = (B_k + B_j) + \mathrm{i}2\eta B_k B_j, \quad r_2 = (B_k + B_j)\eta - \mathrm{i}2, \quad s_1 = 4B_k B_j, \quad s_2 = -\mathrm{i}2(B_k - B_j)^2 \tag{7}$$

It is found that once the set of expansion and Gaussian coefficients from Eq. (3) is obtained, the result from this procedure with use of Eqs. (5)–(7) is considerably simpler to evaluate than the original field integral of Eq. (2b) for the second-harmonic beam, requiring at most numerical integration of one dimension. Computation amount for the sound beam distribution is then greatly reduced [32–34].

3. Bessel beams

A practical Bessel beam (transducer) with a finite extent may be approximately modeled by [8]

$$\bar{q}_1(r) = \begin{cases} J_0(\alpha' r), & 0 \le r \le a \\ 0, & r > a \end{cases} \tag{8}$$

where a is the radius of the Bessel transducer, and the scaling parameter α' is indeed the radial or transverse wavenumber that determines the main lobe width of the Bessel beam. Express the source function (8) in dimensionless form as

$$\bar{q}_1(\xi) = \begin{cases} J_0(\alpha \xi), & 0 \le \xi \le 1 \\ 0, & \xi > 1 \end{cases} \tag{9}$$

Correspondingly, $\alpha = \alpha' a$ represents the dimensionless radial wavenumber and α/π is roughly the lobe number of a Bessel beam within its aperture.

A key problem in the Gaussian expansion technique is how to expand Eq. (9) into a sum of Gaussian functions. This is usually done by using the computer optimization approach [25]. To overcome the time-expenditure and stability problems in this approach, a simple and analytical approach is preferred. To this end, we start directly from the result of Wen and Breazeale [25] for the radiation field of a uniform piston transducer. Mathematically, their work is equivalent to that the circ function of

$$\mathrm{circ}(\xi) = \begin{cases} 1, & 0 \le \xi < 1 \\ 0, & \xi > 1 \end{cases} \tag{10}$$

is decomposed into a series of Gaussian functions [25],

$$\mathrm{circ}(x) = \sum_{k=1}^{n} a_k \exp(-b_k x^2) \tag{11}$$

Here we replace the original coefficients A_k and B_k with a_k and b_k. Two sets of the expansion coefficients of Eq. (11) are presented: one, consisting of 10 pairs of a and b, is listed in Table 1 of [25], the other, consisting of 15 pairs, is listed in Table 1 of [26]. The precision and the usefulness of these data have been fully demonstrated in many examples. From the Bessel–Fourier transform of Eq. (11), an approximate Gaussian expansion of the Bessel function is [30]

$$J_0(x) = \sum_{k=1}^{n} a_k \exp\left(-\frac{x^2}{4b_k}\right) \tag{12}$$

where the coefficients a_k and b_k are the same as those in Eq. (11). By the numerical result of (12), the 15-term Gaussian expansion approximates $J_0(x)$ very well in the interval of about 0–30. Therefore, the finite aperture Bessel source function (9) is represented by

$$\begin{aligned} \bar{q}_1(\xi) &= J_0(\alpha\xi) \times \mathrm{circ}(\xi) \\ &= \sum_{k=1}^{N} A_k \mathrm{e}^{-B_k \xi^2} \end{aligned} \tag{13}$$

In Eq. (13), the new coefficients A_k and B_k are the combination of the known coefficients a_k and b_k:

$$A_k = a_i a_j, \quad B_k = b_i + \alpha^2/4b_j, \tag{14}$$

where the subscripts i and j range from 1 to n and $k = j + n(i-1)$. The whole Gaussian sum with N ($= n^2$) terms approximately covers the source function of a truncated Bessel beam.

For a practical Bessel beam of finite aperture, there are three characteristic parameters governing the behaviors of the beam propagation. The first two parameters are the aperture radius a (or dimensionless ka) of the beam and the radial wavenumber α', or dimensionless α. The third is the depth of field (or the so-called maximum diffraction-free distance)

$$\eta_{\max} = 2/\alpha \tag{15}$$

which is derived by Durnin et al. [1] in the frame of geometric optics. Within this depth, the finite aperture Bessel beam remains the main feature in the case of infinite aperture and exhibits very little diffraction. Outside this range, the beam exhibits considerable diffraction. This argument is true only for the case that the beam has many lobes of the Bessel function on the aperture [1,2,11]. For a few lobes, the Bessel beam, even within its depth of field, loses the "diffraction-free" feature of an ideal Bessel beam and exhibits noticeable diffraction (beam spreading and amplitude drop-off) [8]. In an extreme case ($\alpha \leq 2.405$) where the aperture of a "Bessel" transducer includes only one main lobe, the Bessel function characteristic of the beam profile is fully lost. In this case, the field pattern is nearly similar to that radiated from a simply sported or clamped piston. This paper does not consider these extremes.

Fig. 1 shows the field distribution of a 10-lobe Bessel beam at the fundamental frequency. As expected, this finite aperture Bessel beam has still the main features of the infinite Bessel beam. The radial beam profile is basically that of the Bessel function distribution. In most of the region from the aperture to the critical distance given by Eq. (15), the main lobe width of the beam remains nearly unchanged with the increase of propagation distance. Beyond this range, diffractive spreading becomes considerable.

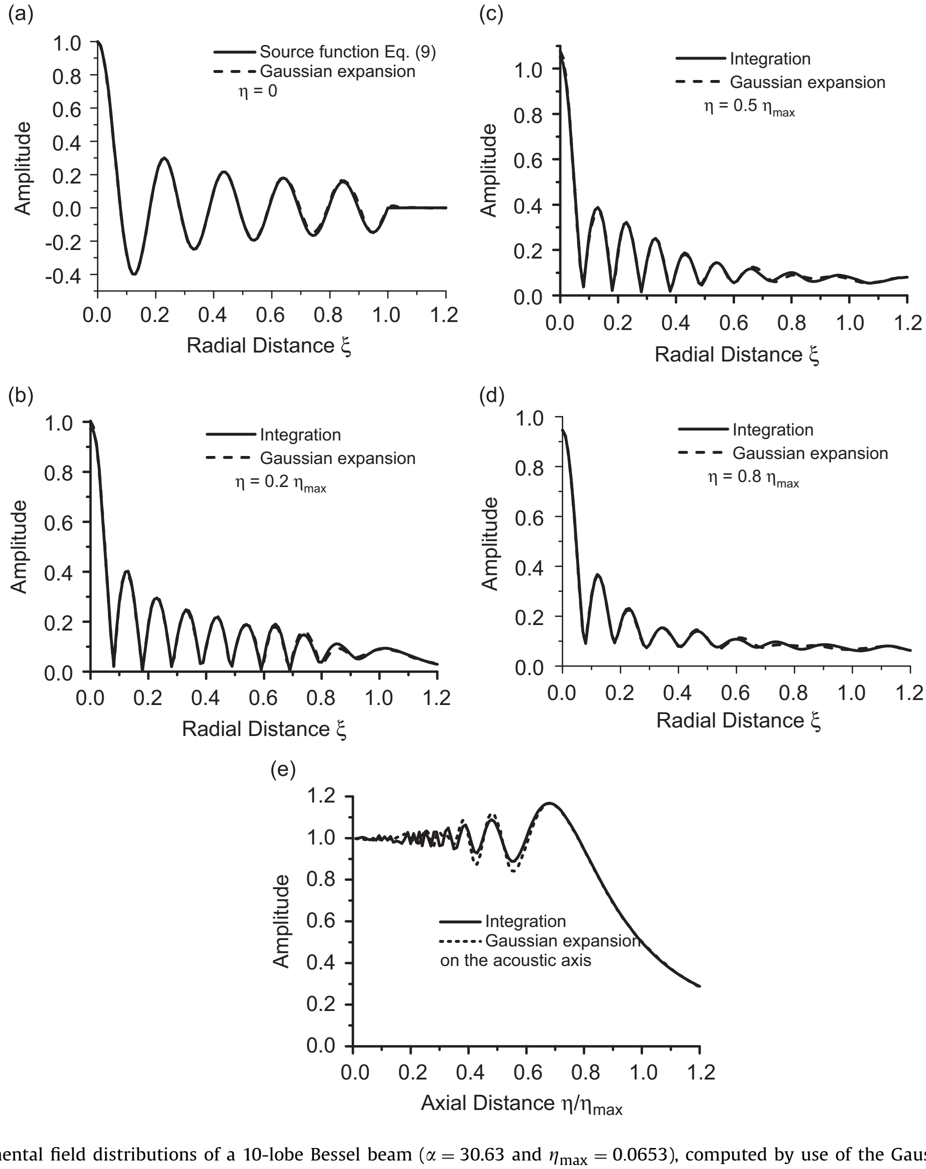

Fig. 1. The fundamental field distributions of a 10-lobe Bessel beam ($\alpha = 30.63$ and $\eta_{max} = 0.0653$), computed by use of the Gaussian expansion. (a) Comparison of approximate source function ($\eta = 0$) of Eq. (13) and the Bessel function of Eq. (9); (b)–(d) are at the axial distance $\eta/\eta_{max} = 0.2$, 0.5 0.8 (within the maximum diffraction-free distance). And (e) is the normalized pressure amplitude on the acoustic axis. To ensure the accuracy of the Gaussian expansion, the results from numerical integration of Eq. (1b) are also graphed here, in fair agreement with these from the Gaussian expansion. In all the calculations, the coefficients in Table 1 of [26] are used.

In the above analysis, we have not considered the influence of absorption by media. In fact, it is obvious that, in the paraxial approximation, the absorption of media only affects the field distribution on the acoustic axis, but does not change the radial beam distribution. (The axial-field is decayed at the exponential term.) In the next section, we will see that, for the second-harmonic generation, the absorption of media will produce effects on the radial distribution of the beam [20]. This relates to the integrand in Eq. (2b).

Before further analysis, let us recall the main features of the second-harmonic component of the ideal infinite-aperture Bessel beam [14–21]. In lossless media, the radial beam profile of the second harmonic is approximated by $J_0^2(\alpha\xi)$ in the near field region of about $0 \le \alpha^2\eta/2 < \pi/2$, and by $J_0(2\alpha\xi)$ in the entire far-field region beyond $\alpha^2\eta/2 \approx 2\pi$. In the transition region of $\pi/2 \le \alpha^2\eta/2 \le 2\pi$, the radial behaviors of the second harmonic deviate slightly from $J_0^2(\alpha\xi)$ and $J_0(2\alpha\xi)$, and the mainlobe width of the beam gradually decreases from approximately $1/\sqrt{2}$ times to one-half times that of the fundamental, as the propagation distance increases. Intuitively, the second harmonic of a practical Bessel beam should also have the properties for the ideal Bessel beam when it propagates within its depth of field. This point of view may be demonstrated by the following numerical calculation.

Fig. 2 shows the second-harmonic field distribution of a 10-lobe Bessel beam in lossless media. The figure indicates that this Bessel beam possesses the same properties as in the ideal case of infinite aperture. In the region around

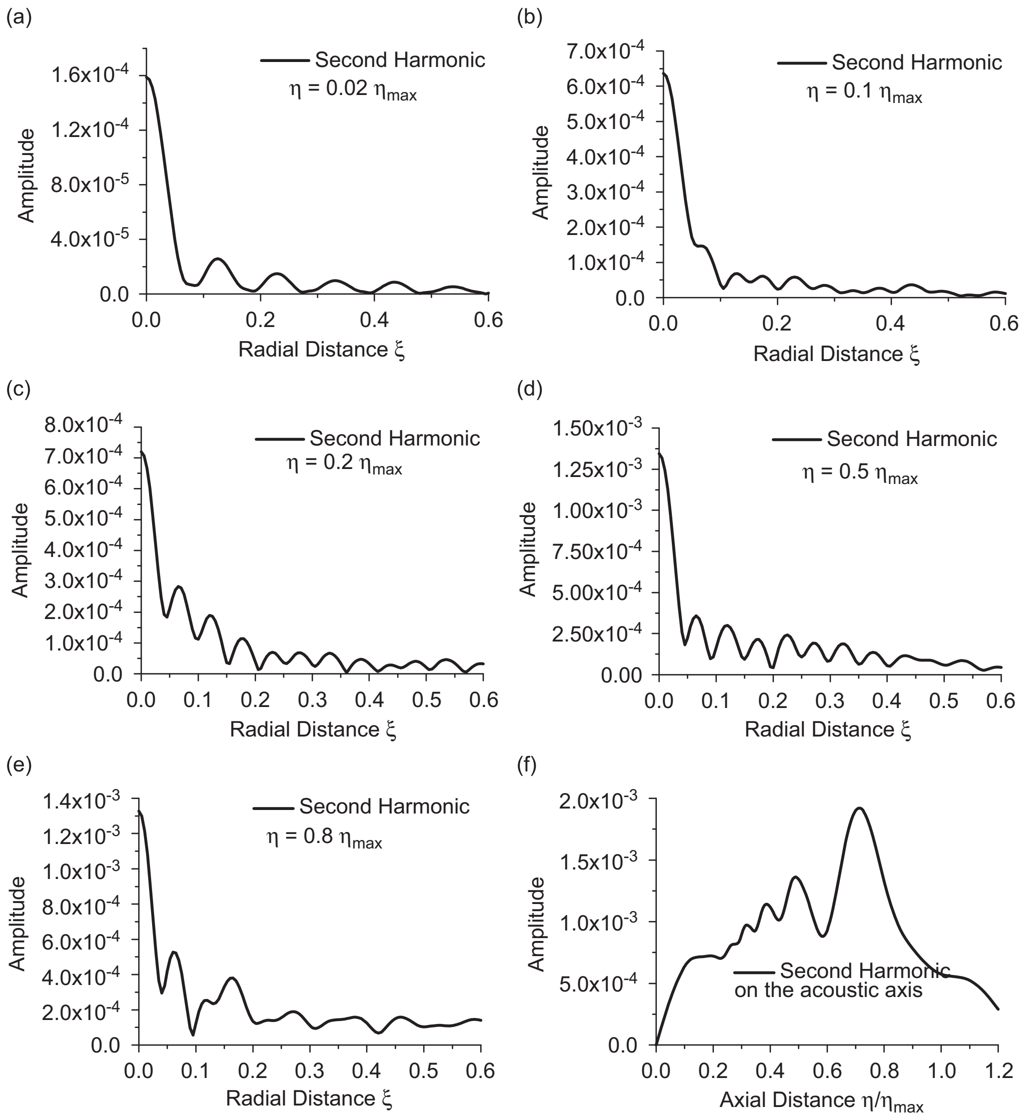

Fig. 2. The second-harmonic field distributions of a 10-lobe Bessel beam, computed by use of the Gaussian expansion. (a)–(e) correspond to the different axial distance $\eta/\eta_{max} = 0.02$, 0.1, 0.2, 0.5, and 0.8. Correspondingly, $\frac{1}{2}\alpha^2\eta = 0.612$ ($<\pi/2$), 3.06, ($<2\pi$), 6.12 ($\approx 2\pi$), 15.3, 24.5 ($>2\pi$). (f) On the acoustic axis ($\xi = 0$). The results here and those in the next Fig. 3 are calculated from the Gaussian expansion method of Eqs. (5)–(7).

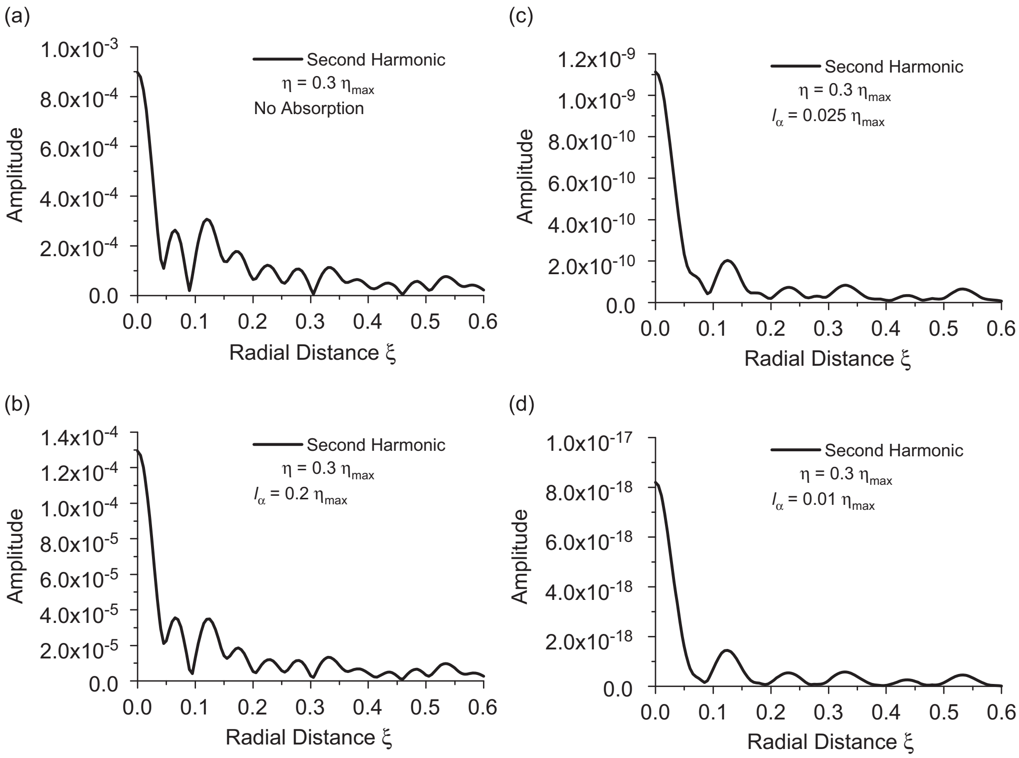

Fig. 3. The far-field beam profiles of the second harmonic with the variation of $\bar{\alpha}\eta_{\max}$. Here $\eta/\eta_{\max} = 0.3$. (a) No absorption; (b)–(d) correspond to the values of $\bar{\alpha}\eta_{\max} = 5$, 40, and 100. In (b), the absorption parameter $\ell_\alpha = 1/\bar{\alpha}$: $\ell_\alpha > \ell_2$. In (c), $\ell_1 < \ell_\alpha < \ell_2$, and in (d) $\ell_\alpha < \ell_1$. In calculation, thermo-viscous fluids are assumed.

$2\pi \leq \alpha^2\eta/2 < \alpha^2\eta_{\max}/2 = \alpha$, the main lobe and the first several sidelobes (profile and beamwidth) in the second-harmonic field are almost independent of the distance of propagation. Their profile is still approximated by the Bessel function $J_0(2\alpha\xi)$ and the width of mainlobe is exactly equal to one-half that at the fundamental frequency, as shown in Figs. 2(c)–(e), and 3(a). In other regions, the beam profile of the second harmonic is basically predicted by the theory from the assumption of infinite aperture.

We now show the influence of absorption on the beam profile of the second harmonic. It is convenient to follow Cunningham and Hamilton [20] and introduce the absorption parameter

$$\bar{\alpha} = \bar{\alpha}_2 - 2\bar{\alpha}_1 \tag{16}$$

and the absorption length $\ell_\alpha = 1/\bar{\alpha}$. We restrict our attention to the case of $\bar{\alpha} > 0$, which corresponds to a fluid for which the absorption coefficient increases to frequency raised to a power greater than unity ($\alpha_\omega \propto \omega^m$, $m > 1$). This criterion includes, for example, thermo-viscous fluids ($m = 2$) and soft tissues ($m \approx 1$) [20]. Here a slight different quantity $\bar{\alpha}\eta_{\max} = (\alpha_2 - 2\alpha_1)z_{\max}$ is used to evaluate how the attenuation of sound affects the radial profile of the second harmonic. The value of this parameter indicates the relative relation between the absorption length and the maximum diffraction-free length. The value of $\bar{\alpha}\eta_{\max} \approx 1$, for example, means that the absorption length is of the same order as the maximum diffraction-free distance. Additionally, the two extremes should be noticed. One is $\alpha_1 = \alpha_2 = 0$ (or $\bar{\alpha}_1 = \bar{\alpha}_2 = 0$) which gives $\bar{\alpha}\eta_{\max} = 0$ naturally. This represents no absorption of media, i.e., an ideal situation. The other is that the absorption coefficients $\alpha_1 \neq 0$ and $\alpha_2 \neq 0$, i.e., the media are absorptive. If these two absorption coefficients are linearly dependent on the frequency of sound ($\alpha_\omega \propto \omega$, then $\alpha_2 = 2\alpha_1$, this corresponds to an "ideal" tissue), then $\bar{\alpha}\eta_{\max} = 0$ also. This fact implies that the absorption parameter $\bar{\alpha}\eta_{\max}$ alone is not sufficient to characterize the propagation behavior of the second harmonic in lossy media and at least one addition parameter is needed.

Fig. 3 is the far-field beam profiles of the second harmonic with a variation of $\bar{\alpha}\eta_{\max}$. It is seen that when the value of $\bar{\alpha}\eta_{\max}$ is relatively small (such as $\bar{\alpha}\eta_{\max} = 5$, $\bar{\alpha}\eta_{\max} = 1$, or smaller), i.e. when the absorption length ℓ_α has the same order of magnitude as the maximum diffraction-free length $\eta_{\max}$, the absorption has no obvious effect on the radial distribution of the second-harmonic beam. The beam profile is still close to an approximate distribution of $J_0(2\alpha\xi)$. For intermediate values of $\bar{\alpha}\eta_{\max}$ (such as $\bar{\alpha}\eta_{\max} = 20$ and $\bar{\alpha}\eta_{\max} = 40$), i.e., the absorption length is roughly located in the transition range, the radial beam distribution of the second harmonic derivates from the distribution $J_0(2\alpha\xi)$ and approaches the transition-range beam profile in the lossless case. For a large value of $\bar{\alpha}\eta_{\max}$, for example $\bar{\alpha}\eta_{\max} = 100$, the absorption length becomes very small so that the far-field beam profile approximates the distribution $J_0^2(\alpha\xi)$ as it is at the near diffraction-free range.

The condition for a relatively small value of the absorption parameter $\bar{\alpha}\eta_{\max}$ means only $\bar{\alpha}_2 \approx 2\bar{\alpha}_1$, but not both $\bar{\alpha}_1$ and $\bar{\alpha}_2$ are small. When $\bar{\alpha}_1$ or $\bar{\alpha}_2$ is large but $\bar{\alpha}\eta_{\max}$ is small, the radial shape in the far diffraction-free range is still similar to the distribution of $J_0(2\alpha\xi)$, not affected by absorption. However, the second-harmonic amplitude is much lower in this range than in the other ranges. In other words, in this case the effective depth of field is much shorter than the depth of field [defined by (15)] in the lossless case. To completely characterize the second-harmonic generation in a practical Bessel beam in lossy media, three parameters are required: maximum diffraction-free distance $\eta_{\max}$, absorption parameter $\bar{\alpha}$, and absorption coefficient absorption $\bar{\alpha}_1$ at the fundamental frequency (or $\bar{\alpha}_2$ at the second-harmonic frequency). The reciprocal of $\bar{\alpha}_1$, $\ell_{\alpha 1} = 1/\bar{\alpha}_1$, represents the dimensionless absorption distance (length) of the fundamental sound (plane) field.

4. Concluding remarks

We conclude this paper by indicating the effective depth of the second-harmonic field of the Bessel beam in lossy media. For a very large absorption parameter $\bar{\alpha}_1$ (it means that a small absorption length $\ell_{\alpha 1} \approx \ell_1$ or even smaller, here $\ell_1 \approx \pi/\alpha^2$), the field depth of the second harmonic is determined by the absorption length $\ell_{\alpha 1}$. In this field depth, the radial beam of $J_0^2(\alpha\xi)$ is predominant. When the value of the absorption parameter $\bar{\alpha}_1$ is intermediate, i.e., when the absorption length is approximately located in the transition range ($\ell_1 < \ell_{\alpha 1} < \ell_2$ and $\ell_2 \approx 4\pi/\alpha^2$), the absorption length $l_{\alpha 1}$ may be viewed as the field depth. The radial profile still has the $J_0^2(\alpha\xi)$ distribution except for small $\bar{\alpha}$ values (correspondingly $\ell_\alpha \gg \ell_2$). When both $\bar{\alpha}_1$ and $\bar{\alpha}$ are small [notice from definition (16) that a small value of $\bar{\alpha}_1$ leads to a small $\bar{\alpha}$], i.e., the corresponding lengths $\ell_{\alpha 1}$ and ℓ_α are both the same order of magnitude as $\eta_{\max}$, or are large compared to $\eta_{\max}$, the second-harmonic field depth is simply the maximum diffraction-free distance $\eta_{\max}$ as defined in lossless case. Furthermore, it is noted that the range from the sound source $\eta = 0$ to the transition distance $\ell_2 \approx 4\pi/\alpha^2$ is just a small portion of the entire depth of field. For a 10-lobe Bessel beam with $\alpha \approx 30$, for instance, $\ell_2/\eta_{\max} \approx 2\pi/\alpha \approx \frac{1}{5}$ is about one-fifth of the entire depth of field. Therefore, it may be reasonable to think that the radial beam shape of the second-harmonic is naturally characterized by the approximate expression $J_0(2\alpha\xi)$ in the entire depth of field. In this sense, we say that the second harmonic of a practical Bessel beam is nearly radially diffraction-free, like its fundamental component. The beam width is exactly equal to one-half that at the fundamental frequency [14–21].

Acknowledgments

One of the authors (J.H.H.) would like to thank the National Science Council of Taiwan (Contract nos. NSC 95-2221-E-035-013-MY3 and 95-2221-E-035-087), which supported this research. The author (D.D.) acknowledges support from the National Natural Science Foundation of China under Grant no. 10674024, and the Natural Science Foundation of Institute of Acoustics, Chinese Academy of Sciences under Grant no. 8506003079.

References

[1] J. Durnin, Exact solutions for nondiffracting beams. I. The scalar theory, *Journal of the Optical Society of America* A4 (1987) 651–654.
[2] J. Durnin, J.J. Miceli, J.H. Eberly, Diffraction-free beams, *Physical Review Letters* 58 (1987) 1499–1501.
[3] G. Indebetouw, Nondiffracting optical fields: some remarks on their analysis and synthesis, *Journal of the Optical Society of America* A6 (1989) 150–152.
[4] A. Vasara, J. Turunen, A.T. Friberg, Realization of general nondiffracting beams with computer-generated holograms, *Journal of the Optical Society of America* A6 (1989) 1748–1754.
[5] R.M. Herman, T.A. Wiggins, Production and uses of diffractionless beams, *Journal of the Optical Society of America* A8 (1991) 932–942.
[6] T. Wulle, S. Herminghaus, Nonlinear optics of Bessel beams, *Physical Review Letters* 70 (1993) 1401–1404.
[7] J. Arlt, K. Dholakia, L. Allen, M.J. Padgett, Efficiency of second-harmonic generation with Bessel beams, *Physical Review E* 60 (1999) 2438–2441.
[8] D.K. Hsu, F.J. Margetan, D.O. Thompson, Bessel beam ultrasonic transducer: fabrication method and experimental results, *Applied Physics Letters* 55 (1989) 2066–2068.
[9] J.A. Compbell, S. Soloway, Generation of a nondiffracting beam with frequency-independent beamwidth, *Journal of the Acoustical Society of America* 88 (1990) 2467–2477.
[10] P.R. Stepanishen, J. Sun, Acoustic bullets: transient Bessel beams generated by planar apertures, *Journal of the Acoustical Society of America* 102 (1997) 3308–3318.
[11] J.-y. Lu, J.F. Greenleaf, Pulse-echo imaging using a nondiffracting beam transducer, *Ultrasound in Medicine and Biology* 17 (1991) 265–281.
[12] J.-y. Lu, 2-D and 3-D high frame rate imaging with limited diffraction beams, *IEEE Transactions on Ultrasonics, Ferroelectrics and Frequency Control* 44 (1997) 839–856.
[13] J.-y. Lu, Experimental study of high frame rate imaging with limited diffraction beams, *IEEE Transactions on Ultrasonics, Ferroelectrics and Frequency Control* 45 (1998) 84–97.
[14] D. Ding, Z. Lu, The second-harmonic component in the Bessel beam, *Applied Physics Letters* 68 (1996) 608–610;
D. Ding, Z. Lu, The second-harmonic component in the Bessel beam, *Applied Physics Letters* 71 (1997) 723–724.
[15] J. Synnevag , S.Holm, Non-linear propagation of limited diffraction beams, *IEEE International Ultrasonics Symposium*, Vol. 2, Sendai, October 1998, pp. 1885–1888.
[16] D. Ding, X. Liu, The second-harmonic generation of a conical sound source, *Journal of the Acoustical Society of America* 104 (1998) 2645–2653.
[17] D. Ding, S. Wang, Y. Wang, Nonlinear propagation of Bessel–Gauss ultrasonic beams, *Journal of Applied Physics* 86 (1999) 1716–1723.
[18] D. Ding, J.-y. Lu, Second-harmonic generation of the *n*th-order Bessel beam, *Physical Review E* 61 (2000) 2038–2041.
[19] D. Ding, J.-y. Lu, Higher-order harmonics of limited diffraction Bessel beams, *Journal of the Acoustical Society of America* 107 (2000) 1212–1214.

[20] K.B. Cunningham, M.F. Hamilton, Bessel beams of finite amplitude in absorbing fluids, *Journal of the Acoustical Society of America* 108 (2000) 519–525.
[21] D. Ding, J. Xu, Y. Wang, Second-harmonic generation of Bessel beams in lossy media, *Chinese Physics Letters* 19 (2002) 689–690.
[22] S. Aanonsen, T. Barkve, J.N. Tjøtta, S. Tjøtta, Distortion and harmonic generation in the nearfield of a finite amplitude sound beam, *Journal of the Acoustical Society of America* 75 (1984) 749–768.
[23] M.F. Hamilton, J.N. Tjøtta, S. Tjøtta, Nonlinear effects in the farfield of a directive sound source, *Journal of the Acoustical Society of America* 78 (1984) 202–216.
[24] M.F. Hamilton, Sound beams, in: M.F. Hamilton, D.T. Blackstock (Eds.), *Nonlinear Acoustics*, Academic Press, Boston, 1998 (Chapter 8).
[25] J.J. Wen, M.A. Breazeale, A diffraction beam field expressed as the superposition of Gaussian beams, *Journal of the Acoustical Society of America* 83 (1988) 1752–1756.
[26] D. Huang, M.A. Breazeale, A Gaussian finite-element method for description of sound diffraction, *Journal of the Acoustical Society of America* 106 (1999) 1771–1781.
[27] D. Ding, X. Liu, Approximate description for Bessel, Bessel–Gauss and Gaussian beams with finite aperture, *Journal of the Optical Society of America A* 16 (1999) 1286–1293.
[28] D. Ding, Y. Zhang, J. Liu, Some extensions of the Gaussian beam expansion: radiation fields of the rectangular and the elliptical transducer, *Journal of the Acoustical Society of America* 113 (2003) 3043–3048.
[29] D. Ding, Y. Zhang, Notes on the Gaussian beam expansion, *Journal of the Acoustical Society of America* 116 (2004) 1401–1405.
[30] D. Ding, X. Tong, P. He, Supplementary notes on the Gaussian beam expansion (L), *Journal of the Acoustical Society of America* 118 (2005) 608–611.
[31] D. Ding, J. Xu, The Gaussian beam expansion applied to Fresnel field integrals, *IEEE Transactions on Ultrasonics, Ferroelectrics and Frequency Control* 53 (2006) 246–250.
[32] D. Ding, Y. Shui, J. Lin, D. Zhang, A simple calculation approach for the second-harmonic sound field generated by an arbitrary axial-symmetric source, *Journal of the Acoustical Society of America* 100 (1996) 727–733.
[33] D. Ding, A simplified algorithm for the second-order sound fields, *Journal of the Acoustical Society of America* 108 (2000) 2759–2764.
[34] D. Ding, A simplified algorithm for second-order sound beams with arbitrary source distribution and geometry, *Journal of the Acoustical Society of America* 115 (2004) 35–37.